ISSN 1070-4272, Russian Journal of Applied Chemistry, 2020, Vol. 93, No. 7, pp. 954–959. © Pleiades Publishing, Ltd., 2020.
Russian Text © The Author(s), 2020, published in Zhurnal Prikladnoi Khimii, 2020, Vol. 93, No. 7, pp. 938–944.

CATALYSIS

Effect of Temperature and Pressure on Conversion of Methane and Lifetime of the Catalyst in the Catalytic Decomposition of Methane

M. V. Popov[a,b,c,*], A. G. Bannov[b], A. E. Brester[b], and P. B. Kurmashov[b]

[a] *Zelinsky Institute of Organic Chemistry of Russian Academy of Sciences, Moscow, 119991 Russia*
[b] *Novosibirsk State Technical University, Novosibirsk, 630073 Russia*
[c] *Mendeleev University of Chemical Technology of Russia, Moscow, 125047 Russia*
**e-mail: popovmaxvik@gmail.com*

Received November 13, 2019; revised February 6, 2020; accepted February 21, 2020

Abstract—The results of studying the effect of temperature and pressure on conversion of methane and the catalyst lifetime during the catalytic decomposition of methane with the formation of hydrogen and nanofibrous carbon on a Ni–Cu catalyst are presented. The pressure varied in the range of 1–10 atm at the temperatures of 600 and 675°C. It was found that when increasing pressure, the total yield of hydrogen increases from the start of synthesis to the deactivation of the catalyst. This effect is manifested the stronger, the higher the temperature of process. It is shown that increasing pressure allows expanding the temperature range of the process without reducing the total yield of useful products.

Keywords: hydrogen energy, nanofibrous carbon, methane-hydrogen mixture, pressure effect, conversion, yield of hydrogen, methane decomposition

DOI: 10.1134/S1070427220070022

Replacing traditional fuels with alternative hydrogen-containing fuel mixtures can increase efficiency and reduce emissions of gas-piston thermal power plants, autonomous power plants, automobile and other types of transport [1, 2]. One of the promising methods for producing pure hydrogen and hydrogen-containing mixtures is the catalytic decomposition of light hydrocarbons [3, 4]. This process is described by the reaction:

$$CH_4 \rightarrow C_{(solid)} + 2H_2,\ \Delta H^\circ = 75.6\ \text{kJ mol}^{-1},$$

which proceeds over the catalyst at temperatures from 500 to 800°C.

In addition to hydrogen, a valuable product is formed during the reaction, carbon nanofibers, which can be used, for example, as a filler in composite materials [5, 6], as a reagent for the synthesis of refractory materials (boron carbide, chromium, zirconium, vanadium, titanium) [7, 8].

Despite a significant number of works devoted to the catalytic decomposition of methane, there is no consensus among researchers on the process conditions, such as the composition of catalyst, temperature, pressure, allowing to obtain maximum yields of reaction products. An analysis of the published data shows that nickel-containing catalysts of various ratios Ni : Me : support (Me is a promoting additive) are mainly used for the process under study, which usually allows to increase the lifetime of nickel catalyst [9], the optimal temperature range of the process established by the researchers is 550–700°C [10–13]. However, there are no comprehensive studies of the effect of pressure on the catalytic decomposition of methane.

The purpose of this work is to expand our understanding of the process of catalytic decomposition of methane into hydrogen and carbon nanofibers, carried out under pressure from 1 to 10 atm at temperatures of 600 and 675°C over a Ni–Cu catalyst.

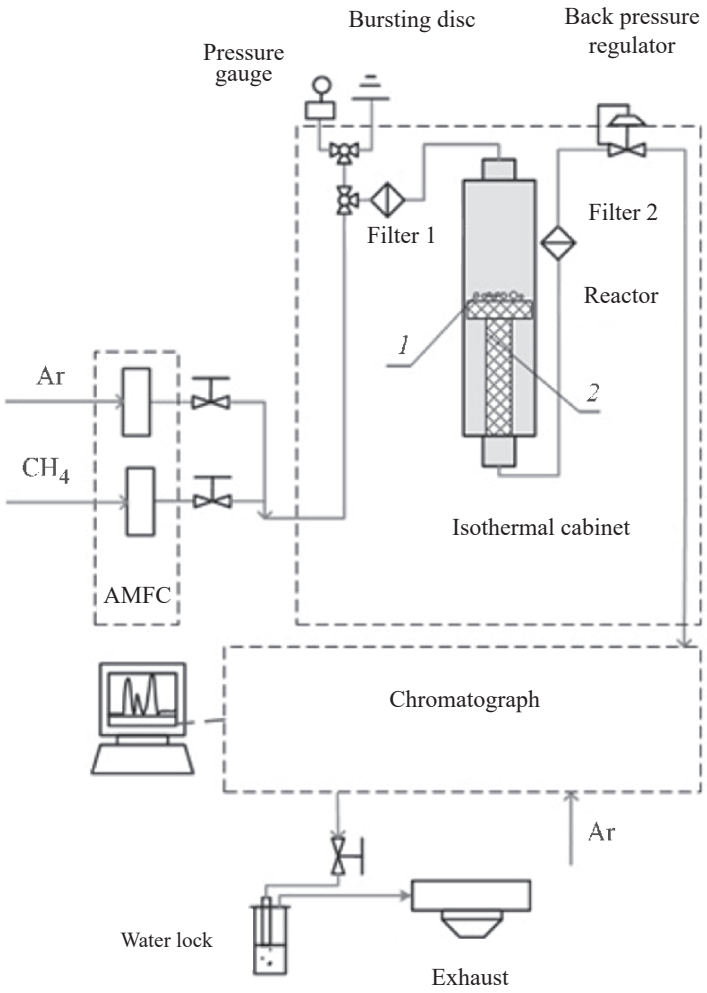

Fig. 1. Schematic diagram of the laboratory setup. (*1*) Catalyst bed, (*2*) quartz substrate.

EXPERIMENTAL

The experiments were performed using an Autoclave Engineers BTRS-Jn flow catalytic system. The scheme of experimental setup is shown in Fig. 1.

Pure methane 99.99 vol % was used as the initial hydrocarbon gas. Gases were supplied to the reactor from cylinders through a reducing valve; the flow rate of the source gas supplied to the reactor was controlled by an automatic multichannel flow controller (AMFC). The reactor was placed in a tubular electric furnace. The temperature was maintained with an accuracy of 1°C. The catalyst fell onto the substrate inside the reactor. The system with a catalyst was heated to a predetermined reaction temperature in argon, followed by switching to methane. The pressure in the system was regulated and controlled with an accuracy of 0.14 atm by a back pressure regulator with a manometer.

The substrate was a quartz glass tube of 210 mm long and a 10 mm external diameter. There was a special partition in the tube where the catalyst was placed, and holes were made in it through which gas penetrated the substrate and interacted with the catalyst.

The main parameters characterizing the thermocatalytic decomposition of methane are: conversion of methane X_{CH_4}, catalyst lifetime t, and specific yield of hydrogen y_{H_2}. Based on the equations of mass balance and data of chromatographic analysis, conversion of methane (%) and specific yield of hydrogen were calculated as follows:

$$X_{CH_4} = \frac{c^0_{CH_4} - c^i_{CH_4}}{c^0_{CH_4}(1 + c^i_{CH_4})} \times 100,$$

$$y_{CH_4} = \frac{M_{H_2}}{M_{H_{cat}}},$$

where $c^0_{CH_4}$ is the initial concentration of methane; $c^i_{CH_4}$ is the current concentration of methane; M_{cat} is the mass of the catalyst; M_{H_2} is the amount of hydrogen resulting from the reaction.

The concentrations of the reaction products in the exhaust gases were measured by gas chromatography on a CHROMOS GC-1000 chromatograph.

The resulting catalyst was investigated using the method of low-temperature nitrogen adsorption on a Quantachrome NOVA 1000e instrument. Before studying the texture characteristics, the samples were degassed in vacuum at 300°C for 6 h to remove physically adsorbed gases and water.

An analysis of the texture properties was carried out at a temperature of 77 K and relative pressures p/p_0 of the adsorbent (nitrogen) gas in the range 0.005–0.995 to construct complete adsorption and desorption isotherms. The specific surface area was calculated by the Brunauer–Emmet–Teller (BET) method. To obtain the size distribution of mesopores, the Barrett–Joyner–Hallenda method was used.

Micrographs of the samples were taken on a Hitachi-3400N scanning electron microscope at an accelerating voltage of 20 kV and a working distance of 10 mm. For registration of images, a secondary electron detector and a backscattered electron detector were used.

Elemental analysis of the samples was performed using an attachment of an energy dispersive spectrometer for scanning electron microscope (Oxford Instruments). EDX spectra were processed by the INCA Energy software. Samples were applied to conductive carbon tape, and stuffed into a mesh for elemental analysis.

The catalyst prepared by the method of alloying metal salts contained, wt %: Ni 82, Cu 8, SiO_2 10.

Initial components for the preparation of the catalyst, such as $Ni(NO_3)_2 \cdot 6H_2O$ (analytical grade) according to State Standard GOST 4055–78, $Cu(NO_3)_2 \cdot 3H_2O$ (analytical grade) according to Technical Specification TU 2622-003- 62931140–2015, ethyl silicate-40 (premium) in accordance with TU 2435-427-05763441-2004, were purchased from OJSC Reaktiv (Novosibirsk).

The required weights of crystalline hydrates of copper and nickel salts were calculated in terms of pure nickel. The salts were mixed in a ceramic cup and slowly heated. When increasing temperature, the salts began to melt in their own crystallization water until a homogeneous mixture was formed. Whenfurther heating of this mixture to a temperature of 150°C, the formation of a solid solution of anhydrous nitrates and their partial decomposition occurred. Then, when the temperature was increased to 400°C (heating rate 15 deg min^{-1}), the final removal of nitrogen oxides was conducted by reactions

$$2Cu(NO_3)_2 \rightarrow 2CuO + 4NO_2 + O_2,$$
$$2Ni(NO_3)_2 \rightarrow 2NiO + 4NO_2 + O_2$$

with the formation of porous, easily crushed structure. The resulting mass was cooled to room temperature with a cooling rate of the furnace and ground to powder.

In the next step, the obtained powder was impregnated with a solution of tetraethoxysilane (ethyl silicate-40) in an organic solvent and the resulting mass was thoroughly mixed. Then this mass was dried at 100°C for 2 h and calcined for 2 h at 400°C, the heating rate was 10 deg min^{-1}. Then, the powder was restored in a hydrogen flow with a flow rate of 50 mL min^{-1} at a temperature of 600°C for 4 h, after which hydrogen was replaced by argon (flow rate 20 mL min^{-1}), and the resulting catalyst was cooled to room temperature.

RESULTS AND DISCUSSION

As the pore diameter of the catalyst decreases, the rate of the process increases until diffusion inhibition takes effect, therewith the decrease in the degree of use of the surface area of catalyst grain was somewhat compensated by the increasing it with diminishing pore diameter [14]. Thus, the activity of catalyst directly depends on the surface area and pore volume. This can be explained by the fact that the activity of the catalyst increases due to the large number of pores and free access of the contacted gas to active sites on the inner surface of the pores in the entire volume of catalyst.

The synthesized catalyst has a high specific surface area of 132 m^2 g^{-1} with a pore volume of 0.13 cm^3 g^{-1}, and the average pore diameter of the catalyst is close to the micropore range (3.9 nm).

From the adsorption isotherm and the type of hysteresis, the type and shape of pores can be one can determined [15, 16]. The hysteresis loop (Fig. 2) of the adsorption and desorption isotherms indicates the presence of mesopores, and the sample has a large number of deaf bottle-shaped pores with very large radii of wide parts and narrow throats. The main part of the catalyst (Fig. 3) is nickel with a small amount of copper, which

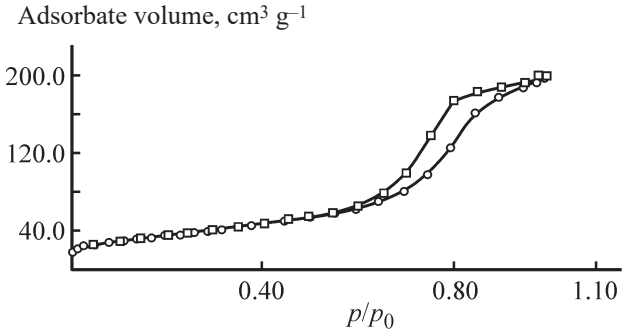

Fig. 2. Adsorption and desorption isotherms of the 82Ni–8Cu/SiO_2 catalyst (wt %).

confirms the expected composition of the samples, the ratio of nickel to copper is ~10 : 1.

The initial conversion of methane was 37% (Fig. 4) at a temperature of 600°C and atmospheric pressure, while the catalyst had a lifetime of 17 h. When increasing the pressure to 10 atm, the initial conversion of methane dropped to 20%, and the catalyst had a lifetime of more than 40 h. When increasing the temperature to 675°C and pressure up to 10 atm, the catalyst lifetime changed insignificantly and amounted to ~40 h (Fig. 4). At a temperature of 675°C, conversion of methane is on average 10% higher than at a temperature of 600°C, and the total maximum yield of hydrogen is 54 mol g_{cat}^{-1} (Fig. 5). Thus, the yield of hydrogen achieved at a pressure of 10 atm during the catalyst deactivation period at 675°C is higher than at 600°C.

It should be noted that the effect of pressure on the total yield of hydrogen manifests itself more significantly at elevated temperatures, when the rate of catalyst deactivation at atmospheric pressure increases sharply. Indeed, at 600°C, the total specific yield of hydrogen does not change significantly with increasing pressure in the region above 3 atm, while at 675°C the specific yield of hydrogen increases by more than 10 times with increasing pressure from atmospheric to 10 atm.

The increase in the total yield of hydrogen can be explained by the fact that, with increasing pressure, the phenomenon of catalyst deactivation is compensated by an increase in the catalyst lifetime. The latter is due to a rise in the partial pressure of hydrogen as a result of an increase in the total pressure, despite the fact that this process is accompanied by a shift in the reaction equilibrium to the left, towards a relative decrease in the hydrogen concentration in the reactor.

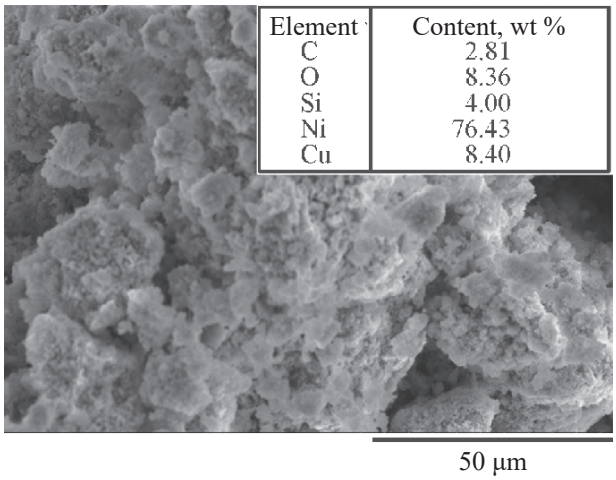

Fig. 3. SEM images of the 82Ni–8Cu/SiO_2 catalyst (wt %) and its elemental composition.

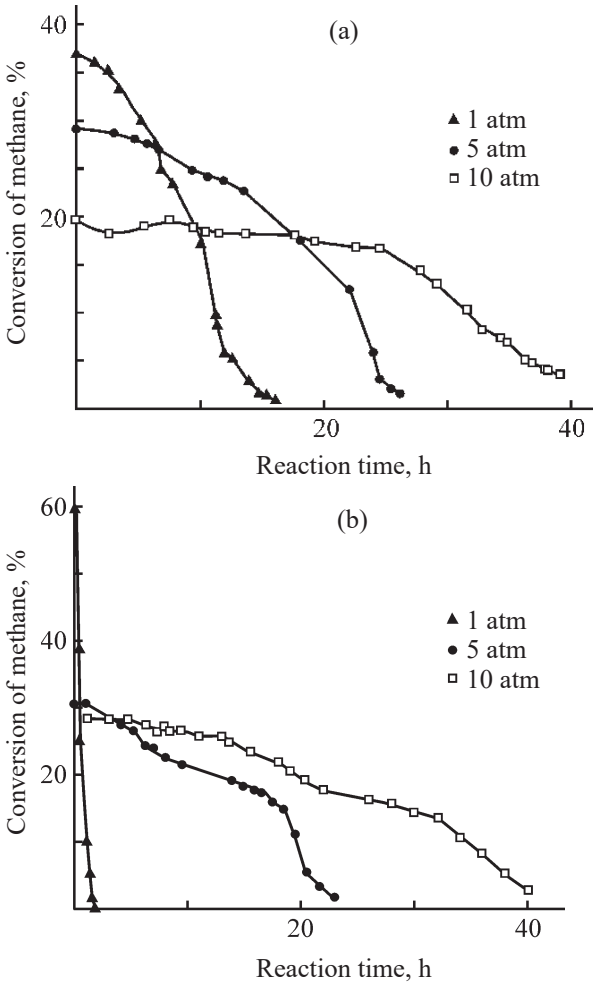

Fig. 4. Conversion of methane vs. the reaction time at various pressures and temperature (a) 600, (b) 675°C.

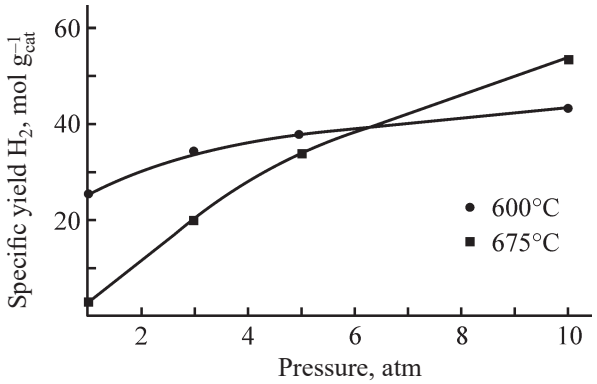

Fig. 5. Specific yield of hydrogen vs. pressure at the temperatures of 600 and 675°C.

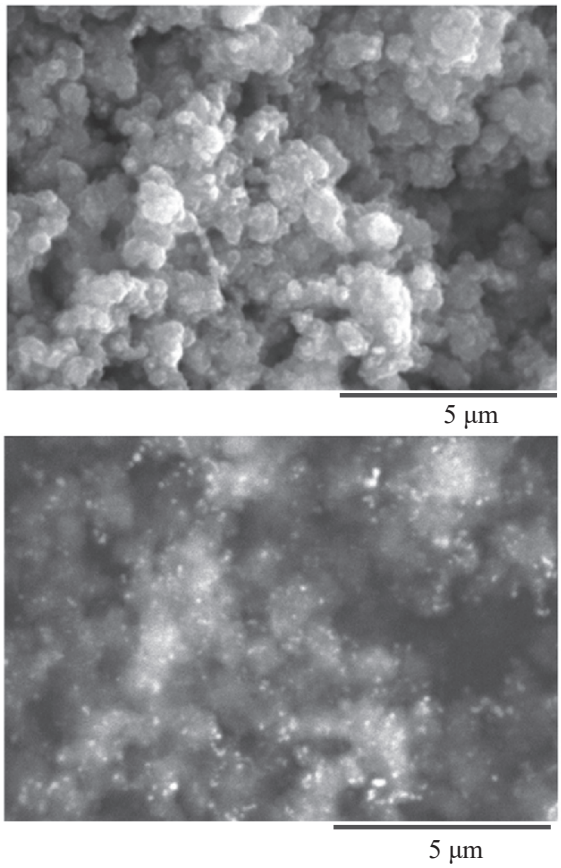

Fig. 6. SEM images of the deactivated catalyst.

It can be expected that a further increase in pressure will make it possible to carry out the process quite efficiently at even higher temperatures, that may be useful from the point of view of controlling the properties of the resulting carbon nanofiber. Indeed, temperature is one of the main parameters affecting the structure and morphology of carbon nanofiber, produced on the basis of the catalytic decomposition of hydrocarbons [17]. However, at atmospheric pressure, the range of temperature variation is limited by the area of intensive deactivation of the catalyst. Obviously, the transition to higher pressures extends the temperature range of effective process proceeding.

During the catalytic decomposition of methane, the catalyst is deactivated due to the encapsulation of the catalyst by the formation of carbon nanofiber on its surface [18]. In the course of the work, electron micrographs of the spent catalyst were obtained (Fig. 6). In the mode of detection of backscattered electrons, it was possible to see particles of a metal catalyst in the bulk of carbon formed. It was shown that the ratio of the formed carbon nanofiber to the amount of catalyst involved is quite large.

CONCLUSIONS

With increasing pressure, the total yield of hydrogen rises for the period of catalyst deactivation during the catalytic decomposition of methane. This effect is manifested the stronger, the higher the process temperature. The method used to prepare the catalyst, the alloying the nickel and copper salts, is technologically simple enough and can be implemented both on a laboratory and industrial scale. It is shown that increasing pressure allows expanding the temperature range of the process without reducing the total yield of useful products.

CONFLICT OF INTEREST

The authors declare no conflict of interest requiring disclosure in this article.

REFERENCES

1. Pevnev, N.G. and Ponamarchuk, V.V., *Vestn. Sib. Gos. Avtomobil'no-dorozhnogo Univ.,* 2017, vol. 55, no. 3, pp. 99–105.
2. Karim, G.A., Wierzba, I., and Al-Alousi, Y., *Int. J. Hydrogen Energy,* 1996, vol. 21, no. 7, pp. 625–621. https://doi.org/10.1016/0360-3199(95)00134-4
3. Kuvshinov, G.G., Mogilnykh, Yu.I., Kuvshinov, D.G., Yermakov, D.Y., Yermakova, M.A., Salanov, A.N., and Rudina, N.A., *Carbon,* 1999, vol. 37, no. 8, pp. 1239–1246. https://doi.org/10.1016/S0008-6223(98)00320-0
4. Ashik, U.P.M., Wan Daud, W.M.A., Abbas, H.F., *Renew Sust. Energ. Rev.,* 2015, vol. 44, pp. 221–256.

https://doi.org/10.1016/j.rser.2014.12.025

5. Bannov, A.G., Uvarov, N.F., Shilovskaya, S.M., and Kuvshinov, G.G., *Nanotechnologies in Russia,* 2012, vol. 7, nos. 3–4, pp. 169–177. https://doi.org/10.1134/S1995078012020048
6. Bannov, A.G., Uvarov, N.F., and Kuvshinov, G.G., *The 8 Int. Forum on Strategic Technologies, IFOST 2013,* vol. 1, pp. 194–199. https://doi.org/10.13140/2.1.1986.0481
7. Krutskii, Y.L., Tyurin, A.G., Popov, M.V., Maksimovskii, E.A., and Netskina, O.V., *Steel in Translation,* 2018, vol. 48, no. 4, pp. 207–213. https://doi.org/10.3103/S096709121804006X
8. Krutskii, Y.L., Popov, M.V., Cherkasova, N.Y., Kvashina, T.S., Chushenkov, V.I., Smirnov, A.I., Felof'yanova, A.V., Aparnev, A.I., Maksimovskii, E.A., and Netskina, O.V.., *Russ. J. Appl. Chem.,* 2018, vol. 91, no. 3, pp. 428–435. https://doi.org/10.1134/S107042721803014X
9. Qian, J.X., Chen, T.W., Enakonda, L.R., Liu, D.B., Mignani, G., Basset, J.-M., and Zhou, L., *Int. J. Hydrogen Energ.,* 2020, vol. 45, no. 15, pp. 7981–8001. https://doi.org/10.1016/j.ijhydene.2020.01.052
10. García-Sancho, C., Guil-López, R., Pascual, L., Maireles-Torres, P., Navarro, R.M., and Fierro, J.L.G., *Appl. Catal. A: General,* 2017, vol. 548, pp. 71–82. https://doi.org/10.1016/j.apcata.2017.07.038
11. Li, J., Gong, Y., Chen, C., Hou, J., Yue, L., Fu, X., Zhao, L., Chen, H., Wang, H., and Peng, S., *Fusion Eng. Des.,* 2017, vol. 125, pp. 593–602. https://doi.org/10.1016/j.fusengdes.2017.05.040
12. Shen, Y. and Lua, A., *Appl. Catal. B: Environmental,* 2015, vol. 164, pp. 61–69. https://doi.org/10.1016/j.apcatb.2014.08.038
13. Li, J., Xiao, C., Xiong, L., Chen, X., Zhao, L., Dong, L., Du, Y., Yang, Y., Wang, H., and Peng, S., *RSC Adv.,* 2016, vol. 6, no. 57, pp. 52154–52163. https://doi.org/10.1039/c6ra05782a
14. Mukhlenov, I.P., Dobkina, E.I., Deryuzhkina, V.I., and Soroko, V.E., *Tekhnologiya katalizatorov* (Catalysits Technology), Leningrad: Khimiya, 1979.
15. Lowell, S., Shields, J.E., Thomas, M.A., and Thommes, M., *Characterization of Porous Solids and Powders: Surface Area, Pore Size and Density,* Netherlands: Springer, 2006. https://doi.org/10.1007/978-1-4020-2303-3
16. Karnaukhov, A.P., *Adsorbtsiya. Tekstura dispersnykh i poristykh materialov* (Texture of Dispersed and Porous Materials), Novosibirsk: Izd. SO RAN, 1999.
17. Ermakova, M.A., Ermakov, D.Yu., Chuvilin, A.L., Kuvshinov, G.G., *J. Catal.,* 2001, vol. 201, no. 2, pp. 183–197. https://doi.org/10.1006/jcat.2001.3243
18. Chesnokov, V.V. and Buyanov, R.A., *Russ. Chem. Rev.,* 2000, vol. 69, no. 7, pp. 623–638. https://doi.org/10.1070/RC2000v069n07ABEH000540